

Supplemental Material to “Spin-Pair Tunneling in Mn₃ Single-Molecule Magnet”

Yan-Rong Li, Rui-Yuan Liu and Yun-Ping Wang

*Beijing National Laboratory for Condensed Matter Physics, Institute of Physics,
Chinese Academy of Sciences, Beijing 100190, People’s Republic of China*

We here present the detailed description of the expected quantum tunnelings, which are labeled from 0 to 16 in Fig.1. Table.1 lists the initial state $|i\rangle$ and the final state $|f\rangle$, the local spin environment (LSE), and tunneling type, and theoretical calculation of resonant field for the quantum tunnelings. $|m\rangle$ and $|m, m\rangle$ stand for the spin states of one single spin and spin pair, where m is the spin quantum number. LSE is labeled as $(n_{\downarrow}, n_{\uparrow})$, where n_{\downarrow} and n_{\uparrow} represent the numbers of spin-down and spin-up spins neighboring to the tunneling spins or spin pairs. SPT and SST are short forms for spin-pair tunneling and single-spin tunneling respectively. $D = 0.98\text{K}$ is the axial anisotropy constant, $J = -0.041\text{K}$ is the intermolecular exchange coupling constant.

TABLE I: The detailed description of the expected quantum tunnelings labeled from 0 to 16 in Fig.1.

n°	$ i\rangle \leftrightarrow f\rangle$	LSE($n_{\downarrow}, n_{\uparrow}$)	Type	Resonant Field
0	$ -6, -6\rangle \leftrightarrow 6, 6\rangle$	(2, 2)	SPT	0
1	$ -6\rangle \leftrightarrow 6\rangle$	(1, 2)	SST	$ J S/g\mu_0\mu_B$
	$ -6\rangle \leftrightarrow 5\rangle$	(3, 0)	SST	$(D - 3 J S)/g\mu_0\mu_B$
	$ -6, -6\rangle \leftrightarrow 6, 6\rangle$	(1, 3)	SPT	$ J S/g\mu_0\mu_B$
2	$ -6, -6\rangle \leftrightarrow 6, 6\rangle$	(0, 4)	SPT	$2 J S/g\mu_0\mu_B$
	$ -6, -6\rangle \leftrightarrow 5, 5\rangle$	(4, 0)	SPT	$(D - 2 J S)/g\mu_0\mu_B$
3	$ -6\rangle \leftrightarrow 6\rangle$	(0, 3)	SST	$3 J S/g\mu_0\mu_B$
	$ -6\rangle \leftrightarrow 5\rangle$	(2, 1)	SST	$(D - J S)/g\mu_0\mu_B$
	$ -6, -6\rangle \leftrightarrow 5, 5\rangle$	(3, 1)	SPT	$3 J S/g\mu_0\mu_B$
4	$ -6, -6\rangle \leftrightarrow 5, 5\rangle$	(2, 2)	SPT	$D/g\mu_0\mu_B$
5	$ -6\rangle \leftrightarrow 5\rangle$	(1, 2)	SST	$(D + J S)/g\mu_0\mu_B$
	$ -6\rangle \leftrightarrow 4\rangle$	(3, 0)	SST	$(2D - 3 J S)/g\mu_0\mu_B$
	$ -6, -6\rangle \leftrightarrow 5, 5\rangle$	(1, 3)	SPT	$(D + J S)/g\mu_0\mu_B$
6	$ -6, -6\rangle \leftrightarrow 5, 5\rangle$	(0, 4)	SPT	$(D + 2 J S)/g\mu_0\mu_B$
	$ -6, -6\rangle \leftrightarrow 4, 4\rangle$	(4, 0)	SPT	$(2D - 2 J S)/g\mu_0\mu_B$
7	$ -6\rangle \leftrightarrow 5\rangle$	(0, 3)	SST	$(D + 3 J S)/g\mu_0\mu_B$
	$ -6\rangle \leftrightarrow 4\rangle$	(2, 1)	SST	$(2D - J S)/g\mu_0\mu_B$
	$ -6, -6\rangle \leftrightarrow 4, 4\rangle$	(3, 1)	SPT	$(2D - J S)/g\mu_0\mu_B$
8	$ -6, -6\rangle \leftrightarrow 4, 4\rangle$	(2, 2)	SPT	$2D/g\mu_0\mu_B$
9	$ -6\rangle \leftrightarrow 4\rangle$	(1, 2)	SST	$(2D + J S)/g\mu_0\mu_B$
	$ -6\rangle \leftrightarrow 3\rangle$	(3, 0)	SST	$(3D - 3 J S)/g\mu_0\mu_B$
	$ -6, -6\rangle \leftrightarrow 4, 4\rangle$	(1, 3)	SPT	$(2D + J S)/g\mu_0\mu_B$
10	$ -6, -6\rangle \leftrightarrow 4, 4\rangle$	(0, 4)	SPT	$(2D + 2 J S)/g\mu_0\mu_B$
	$ -6, -6\rangle \leftrightarrow 3, 3\rangle$	(4, 0)	SPT	$(3D - 2 J S)/g\mu_0\mu_B$
11	$ -6\rangle \leftrightarrow 4\rangle$	(0, 3)	SST	$(2D + 3 J S)/g\mu_0\mu_B$
	$ -6\rangle \leftrightarrow 3\rangle$	(2, 1)	SST	$(3D - J S)/g\mu_0\mu_B$
	$ -6, -6\rangle \leftrightarrow 3, 3\rangle$	(3, 1)	SPT	$(3D - J S)/g\mu_0\mu_B$
12	$ -6, -6\rangle \leftrightarrow 3, 3\rangle$	(2, 2)	SPT	$3D/g\mu_0\mu_B$
13	$ -6\rangle \leftrightarrow 3\rangle$	(1, 2)	SST	$(3D + J S)/g\mu_0\mu_B$
	$ -6\rangle \leftrightarrow 2\rangle$	(3, 0)	SST	$(4D - 3 J S)/g\mu_0\mu_B$
	$ -6, -6\rangle \leftrightarrow 3, 3\rangle$	(1, 3)	SPT	$(3D + J S)/g\mu_0\mu_B$
14	$ -6, -6\rangle \leftrightarrow 3, 3\rangle$	(0, 4)	SPT	$(3D + 2 J S)/g\mu_0\mu_B$
	$ -6, -6\rangle \leftrightarrow 2, 2\rangle$	(4, 0)	SPT	$(4D - 2 J S)/g\mu_0\mu_B$
15	$ -6\rangle \leftrightarrow 3\rangle$	(0, 3)	SST	$(3D + 3 J S)/g\mu_0\mu_B$
	$ -6\rangle \leftrightarrow 2\rangle$	(2, 1)	SST	$(4D - J S)/g\mu_0\mu_B$
	$ -6, -6\rangle \leftrightarrow 2, 2\rangle$	(3, 1)	SPT	$(4D - J S)/g\mu_0\mu_B$
16	$ -6, -6\rangle \leftrightarrow 2, 2\rangle$	(2, 2)	SPT	$4D/g\mu_0\mu_B$

Spin-Pair Tunneling in Mn₃ Single-Molecule Magnet

Yan-Rong Li, Rui-Yuan Liu and Yun-Ping Wang

*Beijing National Laboratory for Condensed Matter Physics, Institute of Physics,
Chinese Academy of Sciences, Beijing 100190, People's Republic of China*

(Dated: August 29, 2018)

We report spin-pair tunneling observed in Mn₃ single-molecule magnet, which is a crystal with 2D network of identical exchange coupling. We observed a series of extra quantum tunnelings by the ac susceptibility measurements, and demonstrated these are concerted tunnelings of two spins taking place from the same initial state to the same final state simultaneously. The resonant field of spin-pair tunneling can be expressed as $H_z = lD/g\mu_0\mu_B + (n_\downarrow - n_\uparrow)JS/2g\mu_0\mu_B$, and the splitting interval ($|J|S/g\mu_0\mu_B$) is half of that of the single-spin tunneling ($2|J|S/g\mu_0\mu_B$), which is analogous to the relationship between the magnetic flux quantum in superconductor ($h/2e$) and common metal (h/e).

PACS numbers: 75.45.+j, 75.50.Xx, 71.10.Li, 75.30.Et

As the counterpart of the electron tunneling, the spin tunneling in single-molecule magnets (SMMs) manifested by the quantum tunneling of the magnetization (QTM) has attracted great interest recently[1–4]. In the existing picture of single-molecule magnets (SMMs), molecules are highly identical and magnetically independent of each other [1–3], hence the spin tunneling of the molecular clusters does not rely on its neighbors. The studies on dimer systems indicate that the intermolecular exchange coupling has the great influence on the performance of QTM, each half of the dimer acts as a field bias on its neighbours, shifting the tunneling resonances to new positions relative to isolated molecules[5–7]. Recent research discovered that for the SMMs with identical exchange coupling (IEC), the quantum tunneling of molecules heavily depends on its local spin environments (LSEs)[9]. In this letter, we report spin-pair tunneling (SPT), which represents the concerted quantum tunneling of two spins taking place from the same initial state to the same final state simultaneously. The two spins appear to form a pair and tunnel as a unit. SPT is clearly identified in the ac susceptibility curves of Mn₃ SMM, and evidenced by the abnormally high effective barrier at zero field as well.

The crystal of Mn₃ SMM has the formula [Mn₃O(Et-sao)₃(MeOH)₃(ClO₄)]. The preparation and crystal characteristics of Mn₃ SMM have been reported in earlier literatures [8, 9]. As described in Ref.[9], Mn₃ SMM is a crystal with 2D network of exchange coupling, in which each molecule is coupled with three neighboring molecules by hydrogen bonds in ab plain, forming a honeycomb-like structure viewed down along the c-axis, therefore Mn₃ SMM are considered to be a crystal with IEC and a model systems of simple Ising model. Each molecule has the ground spin state of $S = 6$ and a spin Hamiltonian of $\hat{H} = -D\hat{S}_z^2 + g\mu_0\mu_B\hat{S}_zH_z$, where $D = 0.98\text{K}$, $g = 2.06$ [8]. Due to the identical exchange coupling in Mn₃ SMM, the quantum tunneling is equally split in the way of $(n_\downarrow - n_\uparrow)JS/g\mu_0\mu_B$, where n_\downarrow and n_\uparrow represent the numbers of spin-down and spin-up molecules neighboring to the tunneling molecule, and

$J = -0.041\text{K}$ is the intermolecular exchange coupling constant[9].

Below the blocking temperature, SMMs show slow magnetic relaxation as spin-flippings become difficult due to the high energy barrier, whereas SMMs show fast magnetic relaxation at the resonant tunneling field because of quantum tunneling effect, which leads to the step-like hysteresis loops[1–4]. Apart from dc susceptibility measurement, ac susceptibility measurement is also considered a good way to define the magnetic relaxation behavior in SMMs. Since the magnetic relaxation time obviously decreases at the resonant tunneling field, ac susceptibility demonstrates the peaks at the resonant tunneling fields[10].

The blocking temperature of Mn₃ SMM is estimated to be 3K [9], hence we measured ac susceptibility at temperatures above 3k. Fig.1(a) shows the field dependence of ac susceptibility at 7K with a frequency of 9.99KHz. A series of peaks and dips have been observed in χ' (real component) and χ'' (imaginary component) curve respectively. Field dependence of χ''/χ' is shown in Fig.1(b), which is considered a quantity proportional to the relaxation times[11], clearly χ''/χ' demonstrates dips at the resonant fields. Apparently, in addition to the quantum tunnelings numbered as 1, 3, 5, 7, 9, 11, 15, which are due to the spin tunneling of single Mn₃ molecule in different spin environments according to Ref.[9], four extra quantum tunnelings numbered as 0, 2, 6, 10, and located at 0T, 0.34T, 1.08T, 1.80T respectively are observed. Here the location of all the resonant fields are temperature and frequency independent. Phenomenally, each of the extra quantum tunneling mentioned above happens to appear at the midpoint between its two neighbor tunnelings. It is also noticeable that, there is a quantum tunneling taking place at zero field. It had been suspected that a different type of isolated molecule might exist, which contributed to the extra tunnelings. However, this conjecture is dismissed, since the four-circle diffraction measurement shows the sample is a good single crystal, and Fig.1 shows that every resonant field of the extra tunnelings is located at the midpoint between

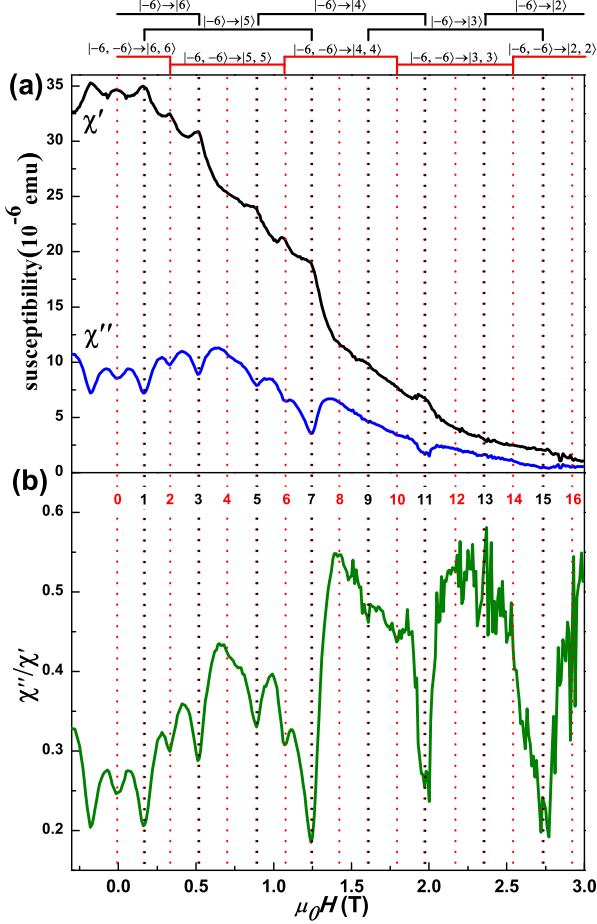


FIG. 1: (Color online). (a) Field dependence of ac susceptibility χ' (real component) and χ'' (imaginary component) from -0.3T to 3T at 7K , with the sweeping rate of 0.001T/s and frequency of 9.99KHz . (b) Field dependence of χ''/χ' from -0.3T to 3T . The quantum tunnelings marked by black and red dotted lines are single-spin tunnelings and spin-pair tunnelings in different quantum tunneling sets, respectively [12].

its two neighboring tunnelings. We will demonstrate in the following that, these extra tunnelings as well as the tunneling occurring at zero field are of spin-pair tunnelings (SPT), i. e. concerted tunneling by two spins taking place from the same initial state to the same final state simultaneously.

In Mn_3 SMM, a single molecule has three exchange-coupled neighbors, hence, a pair of Mn_3 molecules has four exchange-coupled neighbors. Fig.2 demonstrates the five local spin environments (LSEs) of a spin pair marked in black, which is labelled as $(n_\downarrow, n_\uparrow)$ as described in Ref.[9].

For the SMMs with IEC, the spin Hamiltonian of each molecule may be presented as:

$$\hat{H} = -D\hat{S}_z^2 + g\mu_0\mu_B\hat{S}_zH_z - \sum_{i=1}^n J\hat{S}_z\hat{S}_{iz} + \hat{H}^{trans}, \quad (1)$$

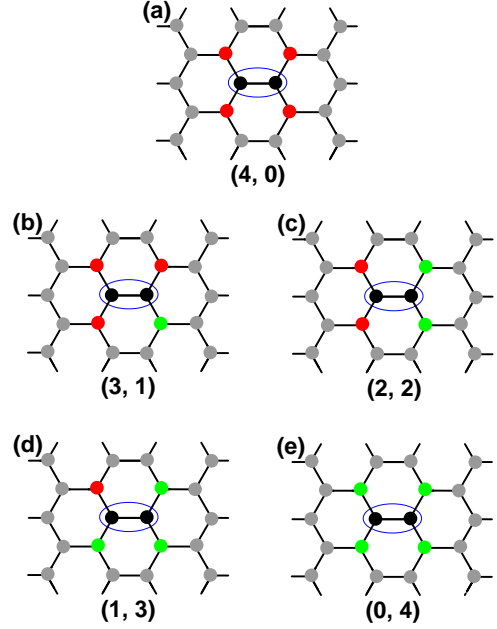


FIG. 2: (Color online). Sketch maps of five spin configurations with different LSE $(n_\downarrow, n_\uparrow)$ for a pair of molecules, other equivalent spin configurations are not listed here for simplicity. The tunneling pair in blue ellipse is marked in black color, which could occupy either spin-up or spin-down state simultaneously. Its four neighboring molecules with red and green color occupy spin-down and spin-up states respectively. The direction of spin is perpendicular to the honeycomb lattice of Mn_3 SMM. The black lines between molecules represent the exchange couplings.

where n is coordination number, \hat{S}_z and \hat{S}_{iz} are the easy-axis spin operators of the molecule and its i th exchange-coupled neighboring molecule, \hat{H}^{trans} is the small off-diagonal perturbation term which allows the quantum tunneling to occur[9]. For the single-spin tunneling (SST) from $|-S\rangle$ to $|S-l\rangle$ ($l = 0, 1, 2, 3, \dots$), the resonant field is determined by

$$H_z = lD/g\mu_0\mu_B + (n_\downarrow - n_\uparrow)JS/g\mu_0\mu_B, \quad (2)$$

and hence the quantum tunneling from $|-6\rangle$ to $|6\rangle$ spin state is split into four, which occurs at $3JS/g\mu_0\mu_B$, $JS/g\mu_0\mu_B$, $-JS/g\mu_0\mu_B$, $-3JS/g\mu_0\mu_B$ respectively[9]. However, for the SPT from $|-S, -S\rangle$ to $|S-l, S-l\rangle$ (the spin state of the pair can be represented as $|m, m\rangle$, where m is the spin quantum number of the two spins in one pair), the resonant field is determined by

$$H_z = lD/g\mu_0\mu_B + (n_\downarrow - n_\uparrow)JS/2g\mu_0\mu_B, \quad (3)$$

and hence the quantum tunneling from $|-6, -6\rangle$ to $|6, 6\rangle$ spin state is split into five, which occurs at $2JS/g\mu_0\mu_B$, $JS/g\mu_0\mu_B$, 0 , $-JS/g\mu_0\mu_B$, $-2JS/g\mu_0\mu_B$ respectively. Apparently the splitting interval of SPT is $|J|S/g\mu_0\mu_B$, which is half of that of SST.

Fig.1 has demonstrated all SSTs and SPTs in different quantum tunneling sets [12], which are marked by black and red dotted lines, respectively. Within a SST set, the LSEs are (3, 0), (2, 1), (1, 2), (0, 3) from the left to the right, respectively, and within a SPT set, the LSEs are (4, 0), (3, 1), (2, 2), (1, 3), (0, 4) from the left to the right, respectively.

Since the axial anisotropy constant $D = 0.98\text{K}$ happens to be close to $4|J|S$ in Mn_3 SMM [9, 13], there are quantum tunnelings overlapping, for example, the quantum tunneling numbered as 1 is the combinations of the SST from $|-6\rangle$ to $|6\rangle$ spin state with LSE (1, 2) and the SST from $|-6\rangle$ to $|5\rangle$ spin state with LSE (3, 0) and the SPT from $|-6, -6\rangle$ to $|6, 6\rangle$ spin state with LSE (1, 3). With such coincidence, the quantum tunnelings are taking place at fields with equal interval, just as that happens to the individual SMMs[1, 4]. Of the overlapped tunnelings mentioned above, the contribution of the component quantum tunnelings are different due to the dependence of tunneling on the local spin environment and the potential barrier. It is noticed that the extra quantum tunnelings numbered with even numbers are purely SPT, while the quantum tunnelings numbered with odd numbers are of the combination of SST and SPT. As described in Ref.[9]: the tunneling magnitude \mathcal{T} of SST is

described as:

$$\mathcal{T} = \alpha N_{(n_{\downarrow}, n_{\uparrow})} P_{|m_i\rangle \rightarrow |m_f\rangle}, \quad (4)$$

where $N_{(n_{\downarrow}, n_{\uparrow})}$ is the number of molecules with LSE $(n_{\downarrow}, n_{\uparrow})$, $P_{|m_i\rangle \rightarrow |m_f\rangle}$ is the tunneling probability of the molecule from the spin state $|m_i\rangle$ to $|m_f\rangle$, which is exponentially dependent on the effective barrier at the thermally activated tunneling region[10, 14]. Note that Eq.(4) is applicable to SPT with the following transformation:

$$\mathcal{T} = \alpha N_{(n_{\downarrow}, n_{\uparrow})} P_{|m_i, m_i\rangle \rightarrow |m_f, m_f\rangle}, \quad (5)$$

where $N_{(n_{\downarrow}, n_{\uparrow})}$ is the number of spin pairs with the LSE $(n_{\downarrow}, n_{\uparrow})$, and $P_{|m_i, m_i\rangle \rightarrow |m_f, m_f\rangle}$ is determined by the aggregated effective barrier of two SSTs, which can be deduced from $P_{|m_i, m_i\rangle \rightarrow |m_f, m_f\rangle} \propto P_{|m_i\rangle \rightarrow |m_f\rangle}^2$ and $P_{|m_i\rangle \rightarrow |m_f\rangle} \propto \exp(-U_{eff}/k_B T)$. Apparently, the effective barrier of SPT is doubled, and hence much higher than that of SST, therefore, the tunneling magnitude of SPT is much smaller than SST, and it is of no surprise that only the quantum tunnelings of SST are observed in hysteresis loop at 2K[9]. According to Eq. (4) and (5), the tunneling magnitudes of SST and SPT are heavily dependent on the numbers of single spins and spin pairs in the proper LSEs respectively. At a high positive field, most molecules occupy $|6\rangle$ spin state, therefore SSTs with LSE (0, 3) are phenomenal, such as the quantum tunnelings numbered as 7, 11, 15 observed in Fig.1. On the other hand, only SPTs with LSE (0, 4) are observed at high field, such as the quantum tunnelings numbered as 6, 10 in Fig.1, and the expected quantum tunnelings numbered as 4, 8, 12, 13, 16 are not observed due to very small $N_{(n_{\downarrow}, n_{\uparrow})}$, whereas the absence of SPT numbered as 14 is due to small signal-to-noise ratio.

Fig.3(a) shows ac susceptibility of Mn_3 as a function of temperature with different frequencies, which demonstrates typical characteristic of SMMs: The dissipation peak in $\chi''-T$ curve drops to lower temperature at higher frequency[15–17]. Fig.3(b) shows the fitting of the Arrhenius equation, which gives the effective barrier $U_{eff} = 55\text{K}$, in good agreement with the result mentioned in Ref[8]. It is remarkable that $U_{eff} = 55\text{K}$ is much larger than the anisotropy barrier $DS_z^2 = 35\text{K}$, whereas U_{eff} is usually smaller than DS_z^2 in the previous SMM studies[10, 14]. As mentioned above, the effective barrier of SPT is supposed to be the double of that of SST, and since $U_{eff} = 55\text{K}$ happens to be close to the double of the energy gap (26K) between $|\pm 6\rangle$ and $|\pm 3\rangle$. It is evident that SPT leads to the observed tunneling at zero field, i. e. the spin relaxation at zero field should be dominated by two concerted spin flippings, and each flipping is of thermally assisted tunneling[10]. As shown in the inset of Fig.3(b), the spin pair is initially thermally activated from $|-6, -6\rangle$ state to $|-3, -3\rangle$ state, next tunnels to $|3, 3\rangle$ state, and finally relaxes to $|6, 6\rangle$ state, this is similar to the relaxation process in the previous SMMs studies[10, 14]. Note that quantum tunneling taking place from $|-3, -3\rangle$ to $|3, 3\rangle$ state in this relaxation

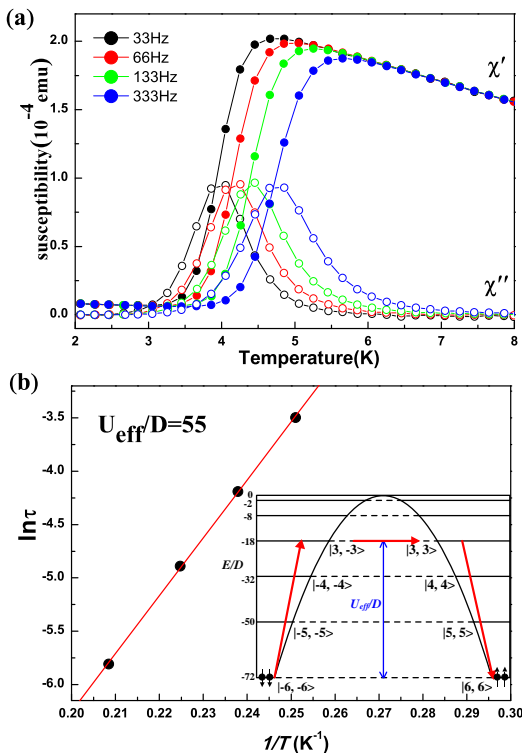


FIG. 3: (Color online). (a) Temperature dependence of ac susceptibility at different frequencies. (b) plot of $\ln(\tau)$ vs $1/T$ with data obtained from ac susceptibility measurement, which gives $U_{eff}/D = 55$, the inset shows the schematic drawing for the magnetic relaxation process within temperature range 4~5K.

TABLE I: The similarities and differences between spin-pair tunneling and Josephson effect.

	spin-pair tunneling	Josephson effect
tunneling unit	spin pair	Cooper pair
pairing partner	not fixed	not fixed
internal state of pair	exchange-energy entanglement state	momentum and spin entanglement state
invariant of pair	net exchange energy is a constant	both net momentum and net spin are zero
tunneling variable	spin orientation of spin pair	position of Cooper pair
relationship with single particle	splitting interval $ J S/g\mu_0\mu_B$ is half of that of the single-spin tunneling ($2 J S/g\mu_0\mu_B$)	quantum flux $h/2e$ is half of that in common metal (h/e)

process is consistent with the selection rule of C_3 symmetry in Mn_3 SMM ($\Delta m_s = 3n$) [18].

SPT in Mn_3 SMM is analogous to the tunneling of superconducting Cooper pairs, i.e. Josephson effect in superconductor, in the sense of that, the two spins of a spin pair entangle to behave as a unit, while the pairing could be formed between a spin and any rather than a particular one of its neighboring spins. It is well known that both the net momentum and spin of the Cooper pairs are zero regardless of the value of the individual momentum and spin, which can be considered as a source of momentum and spin entanglement state[19, 20]. Similarly, the net exchange energy of spin pair is a constant regardless of the individual exchange energy distribution, for example, the SPT at zero field requires the LSE of spin pairs to be (2, 2), which means the net exchange interaction between the spin pair and its neighbors equals to zero, nevertheless there are six equivalent spin distribu-

tions (Fig.2 (c) only shows one of them). Furthermore, the splitting interval of SPT is $|J|S/g\mu_0\mu_B$ according to Eq. (3), which is half of that of SST ($2|J|S/g\mu_0\mu_B$), this is similar to the relationship between the magnetic flux quantum in superconductor($h/2e$) and common metal (h/e). The similarities and differences between SPT and Josephson effect are shown in Table.1. It is notable that spin-pair tunneling is attributed to the identical exchange coupling between the molecules, and hence cannot be observed in the SMMs without exchange coupling such as Mn_{12} [1, 10], Fe_8 [3], etc. To the best of our knowledge, this is the first time that the spin-pair tunneling is observed and reported, which not only adds to the diversity of QTM, but also opens up new perspectives in the quantum physics and potential applications of these molecular nanomagnets.

This work was supported by the National Key Basic Research Program of China (No.2011CB921702).

-
- [1] J. R. Friedman, M. P. Sarachik, J. Tejada, and R. Ziolo, Phys. Rev. Lett. **76**, 3830 (1996).
- [2] L. Thomas, F. Lioni, R. Ballou, D. Gatteschi, R. Sessoli, and B. Barbara, Nature **383**, 145 (1996).
- [3] C. Sangregorio, T. Ohm, C. Paulsen, R. Sessoli, and D. Gatteschi, Phys. Rev. Lett. **78**, 4645 (1997).
- [4] K. L. Taft, C. D. Delfs, G. C. Papaefthymiou, S. Foner, D. Gatteschi, and S. J. Lippard, J. Am. Chem. Soc. **116**, 823 (1994).
- [5] W. Wernsdorfer, N. Aliaga-Alcalde, D. N. Hendrickson, and G. Christou, Nature **416**, 406 (2002).
- [6] W. Wernsdorfer, S. Bhaduri, R. Tiron, D. N. Hendrickson, and G. Christou, Phys. Rev. Lett. **89** 197201 (2002).
- [7] R. Tiron, W. Wernsdorfer, N. Aliaga-Alcalde, and G. Christou, Phys. Rev. B **68** 140407(R) (2003).
- [8] R. Inglis, L. F. Jones, G. Karotsis, A. Collins, S. Parsons, S. P. Perlepes, W. Wernsdorfer, and E. K. Brechin, Chem. Commun., 5924 (2008).
- [9] Y. R. Li, R. Y. Liu, H. Q. Liu, and Y. P. Wang, Phys. Rev. B **89**, 184401 (2014).
- [10] F. Luis, J. Bartolome, J. F. Fernandez, J. Tejada, J. M. Hernandez, X. X. Zhang, and R. Ziolo, Phys. Rev. B **55**, 11448 (1997).
- [11] T. Pohjola, H. Schoeller, Phys. Rev. B **62**, 15026 (2000).
- [12] See Supplemental Material at[] for the detailed description of the expected quantum tunnelings labeled from 0 to 16 in Fig.1.
- [13] R. Inglis, S. M. Taylor, L. F. Jones, G. S. Papaefstathiou, S. P. Perlepes, S. Datta, S. Hill, W. Wernsdorfer, and E. K. Brechin, Dalton Trans. 9157 (2009).
- [14] Y. R. Li, H. Q. Liu, Y. Liu, S. K. Su, and Y. P. Wang, Chin. Phys. Lett. **26**, 077504 (2009).
- [15] A. M. Gomes, M. A. Novak, R. Sessoli, A. Caneschi, and D. Gatteschi, Phys. Rev. B **57**, 5021 (1998).
- [16] X. X. Zhang, J. M. Hernandez, E. del Barco, J. Tejada, A. Roig, E. Molins, and K. Wieghardt, J. Appl. Phys. **85**, 5633 (1999).
- [17] S. Accorsi, et al., J. Am. Chem. Soc. **128**, 4742 (2006).
- [18] J. J. Henderson, C. Koo, P. L. Feng, E. del Barco, S. Hill, I. S. Tupitsyn, P. C. E. Stamp, and D. N. Hendrickson, Phys. Rev. Lett. **103**, 017202 (2009).
- [19] J. Bardeen, L. N. Cooper, and J. R. Schrieffer, Phys. Rev. **108**, 1175 (1957).
- [20] A. Hayat, H-Y. Kee, K. S. Burch, and A. M. Steinberg, Phys. Rev. B **89**, 094508 (2014).